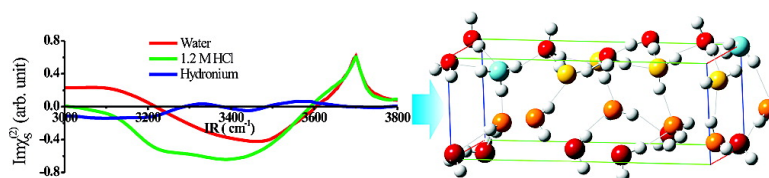


## Interfacial Structures of Acidic and Basic Aqueous Solutions

Chuanshan Tian, Na Ji, Glenn A. Waychunas, and Y. Ron Shen

*J. Am. Chem. Soc.*, **2008**, 130 (39), 13033-13039 • DOI: 10.1021/ja8021297 • Publication Date (Web): 06 September 2008

Downloaded from <http://pubs.acs.org> on February 8, 2009



### More About This Article

Additional resources and features associated with this article are available within the HTML version:

- Supporting Information
- Access to high resolution figures
- Links to articles and content related to this article
- Copyright permission to reproduce figures and/or text from this article

[View the Full Text HTML](#)

## Interfacial Structures of Acidic and Basic Aqueous Solutions

Chuanshan Tian,<sup>†</sup> Na Ji,<sup>†</sup> Glenn A. Waychunas,<sup>‡</sup> and Y. Ron Shen<sup>\*†</sup>*Department of Physics, University of California, Berkeley, California 94720, and Earth Sciences Division, Lawrence Berkeley National Laboratory, Berkeley, California 94720*

Received March 21, 2008; E-mail: yrshen@berkeley.edu

**Abstract:** Phase-sensitive sum-frequency vibrational spectroscopy was used to study water/vapor interfaces of HCl, HI, and NaOH solutions. The measured imaginary part of the surface spectral responses provided direct characterization of OH stretch vibrations and information about net polar orientations of water species contributing to different regions of the spectrum. We found clear evidence that hydronium ions prefer to emerge at interfaces. Their OH stretches contribute to the “ice-like” band in the spectrum. Their charges create a positive surface field that tends to reorient water molecules more loosely bonded to the topmost water layer with oxygen toward the interface, and thus enhances significantly the “liquid-like” band in the spectrum. Iodine ions in solution also like to appear at the interface and alter the positive surface field by forming a narrow double-charge layer with hydronium ions. In NaOH solution, the observed weak change of the “liquid-like” band and disappearance of the “ice-like” band in the spectrum indicates that OH<sup>-</sup> ions must also have excess at the interface. How they are incorporated in the interfacial water structure is, however, not clear.

## Introduction

Water/vapor interfaces of acidic and basic aqueous solutions play a key role in environmental chemistry and atmospheric science.<sup>1,2</sup> They have been the topics of extensive theoretical and experimental studies in recent years,<sup>3–8</sup> but good understanding of the water interfacial structure at the molecular level is still lacking. The most interesting question is whether H<sup>+</sup> and OH<sup>-</sup> ions would emerge at the interface and affect the interfacial hydrogen-bonding network of water. Molecular dynamics (MD) simulations predicted that protons (H<sup>+</sup>) could appear at the interface in the form of hydronium (H<sub>3</sub>O<sup>+</sup>), but OH<sup>-</sup> should be repelled from the water surface.<sup>3,9–12</sup> The details, such as the depth profile of ion concentrations, depend very much on the molecular model and interaction potentials assumed.<sup>9–12</sup> Experiments carried out with scanning tunneling microscopy (STM),<sup>13</sup> X-ray spectroscopy,<sup>14,15</sup> and attenuated total reflection (ATR)<sup>8</sup> have been used to verify the theoretical

prediction. However, they suffer from either the water surface being too dynamic or the techniques not being sufficiently surface-specific.

Sum-frequency vibrational spectroscopy (SFVS) has been proven to be a highly surface-specific and versatile probe for liquid interfaces and is the only technique available to acquire surface vibrational spectra of liquids.<sup>5,6,16</sup> Using SFVS, several research groups have successfully obtained vibrational spectra of water/vapor interfaces of acid, basic, and salt solutions.<sup>5–8,17,18</sup> In all cases, the SFVS spectrum appears to roughly consist of three spectral features in the OH stretch region: a relatively sharp peak at 3700 cm<sup>-1</sup> attributed to the dangling OH protruding at the surface, and two broad bands at ~3200 and ~3450 cm<sup>-1</sup> from bonded OH often labeled as ice-like and liquid-like bands, respectively.<sup>16</sup> When the acid concentration in water was sufficiently high (pH ≤ 2 with HCl), strong enhancement of both ice-like and liquid-like bands was observed.<sup>7,8,11,18</sup> The appearance of hydronium ions at the surface has been used to explain the enhancement.<sup>7,8,11</sup> In basic solution, the liquid-like band displayed slight changes when pH is sufficiently high (pH ≥ 13).<sup>7</sup> It was believed that at high pH, OH<sup>-</sup> anions might have emerged at the interface with enough concentration to distort the interfacial hydrogen-bonding network of water.<sup>7</sup> Salt solutions have also been investigated. Results showed that ions

<sup>†</sup> University of California.<sup>‡</sup> Lawrence Berkeley National Laboratory.

- (1) *The Chemistry of Acid Rain: Sources and Atmospheric Processes*; American Chemical Society: Washington, DC, 1987.
- (2) Irwin, J. G.; Williams, M. L. *Environ. Pollut.* **1988**, *50*, 29–59.
- (3) Jungwirth, P.; Tobias, D. J. *Chem. Rev.* **2006**, *106*, 1259–1281.
- (4) Chang, T. M.; Dang, L. X. *Chem. Rev.* **2006**, *106*, 1305–1322.
- (5) Shen, Y. R.; Ostroverkhov, V. *Chem. Rev.* **2006**, *106*, 1140–1154.
- (6) Gopalakrishnan, S.; Liu, D. F.; Allen, H. C.; Kuo, M.; Shultz, M. J. *Chem. Rev.* **2006**, *106*, 1155–1175.
- (7) Tarbuck, T. L.; Ota, S. T.; Richmond, G. L. *J. Am. Chem. Soc.* **2006**, *128*, 14519–14527.
- (8) Levering, L. M.; Sierra-Hernandez, M. R.; Allen, H. C. *J. Phys. Chem. C* **2007**, *111*, 8814–8826.
- (9) Dang, L. X. *J. Chem. Phys.* **2003**, *119*, 6351–6353.
- (10) Petersen, M. K.; Iyengar, S. S.; Day, T. J. F.; Voth, G. A. *J. Phys. Chem. B* **2004**, *108*, 14804–14806.
- (11) Mucha, M.; Frigato, T.; Levering, L. M.; Allen, H. C.; Tobias, D. J.; Dang, L. X.; Jungwirth, P. *J. Phys. Chem. B* **2005**, *109*, 7617–7623.
- (12) Ishiyama, T.; Morita, A. *J. Phys. Chem. A* **2007**, *111*, 9277–9285.
- (13) Allongue, P. *Phys. Rev. Lett.* **1996**, *77*, 1986–1989.

- (14) Cappa, C. D.; Smith, J. D.; Messer, B. M.; Cohen, R. C.; Saykally, R. J. *J. Phys. Chem. B* **2006**, *110*, 1166–1171.
- (15) Cappa, C. D.; Smith, J. D.; Messer, B. M.; Cohen, R. C.; Saykally, R. J. *J. Phys. Chem. A* **2007**, *111*, 4776–4785.
- (16) Du, Q.; Superfine, R.; Freysz, E.; Shen, Y. R. *Phys. Rev. Lett.* **1993**, *70*, 2313–2316.
- (17) Baldelli, S.; Schnitzer, C.; Shultz, M. J.; Campbell, D. J. *J. Phys. Chem. B* **1997**, *101*, 10435–10441.
- (18) Baldelli, S.; Schnitzer, C.; Shultz, M. J. *Chem. Phys. Lett.* **1999**, *302*, 157–163.

of small size like to stay in the bulk, while negative ions with large radius such as  $\text{Br}^-$  and  $\text{I}^-$  prefer to stay close to the surface.<sup>6</sup>

How the water interfacial structure would change upon emergence of various types of ions at the water/vapor interface is, however, still not clear. Interpretation of the SF spectrum for the same interface often varies from group to group. The problem arises because the conventional SFVS yields only an intensity spectrum, proportional to the absolute square of the surface nonlinear susceptibility,  $|\chi_S^{(2)}(\omega_{\text{IR}})|^2$ , with  $\chi_S^{(2)}(\omega_{\text{IR}})$  being complex. To deduce information on resonances from  $|\chi_S^{(2)}(\omega_{\text{IR}})|^2$ , one usually assumes discrete resonances and fits the spectrum.<sup>6–8,19</sup> Unfortunately, such fitting is often not unique. The reason is that OH stretch resonances of a water interface are not discrete. They form a broad continuum because of the existence of widely varying geometry and strength of hydrogen bonds connecting interfacial water molecules to their neighbors. Properly characterizing the continuum resonances from fitting of  $|\chi_S^{(2)}(\omega_{\text{IR}})|^2$  is generally not possible. One could approximate the continuum resonances by discrete resonances, but without specifying a priori the resonance frequencies and the signs of their resonant amplitudes, the fitting would not be unique. Thus, when different groups fit the same SF intensity spectrum for a water interface with discrete resonances, they often obtained different results and, accordingly, different interpretations.<sup>7,8</sup> Obviously the situation calls for a direct measurement of  $\text{Im} \chi_S^{(2)}(\omega_{\text{IR}})$ , which, playing the same role as the imaginary part of the dielectric constant for absorption or emission spectroscopy, contains the desired resonant information.

We have recently developed a phase-sensitive (PS) SFVS technique that allows us to measure spectra of both the amplitude and the phase of  $\chi_S^{(2)}(\omega_{\text{IR}})$ , and hence the spectra of  $\text{Re} \chi_S^{(2)}(\omega_{\text{IR}})$  and  $\text{Im} \chi_S^{(2)}(\omega_{\text{IR}})$ .<sup>20,21</sup> We have applied it to the neat water/vapor interface and obtained a more detailed understanding on the structure of the interface.<sup>22</sup> We can now use the neat water/vapor interface as a reference in our SFVS study of water/vapor interfaces of acid and base solutions. From the spectral changes resulting from dissolving acid or base into water, we can learn how various types of ions appearing at the interface can perturb the interfacial water structure. We shall focus on the  $\text{Im} \chi_S^{(2)}(\omega_{\text{IR}})$  spectra of HCl, NaOH, and HI solutions in which protons, hydroxyls, and iodine ions like to come to the interface.

### Background of Phase-Sensitive Sum-Frequency Vibrational Spectroscopy

Consider two input beams overlapping at a surface, one at a fixed visible frequency and the other tunable over vibrational resonances in the infrared. The SF output is given by  $I(\omega_{\text{SF}}) \propto |\chi_{\text{eff}}^{(2)}|^2$ , with:<sup>23</sup>

$$\chi_{\text{eff}}^{(2)} = [\vec{L}(\omega_{\text{SF}}) \cdot \hat{e}(\omega_{\text{SF}})] \cdot \vec{\chi}_S^{(2)} : [\hat{e}(\omega_{\text{vis}}) \cdot \vec{L}(\omega_{\text{vis}})] [\hat{e}(\omega_{\text{IR}}) \cdot \vec{L}(\omega_{\text{IR}})] \quad (1)$$

where  $\vec{\chi}_S^{(2)}$  is the surface nonlinear susceptibility, and  $\vec{L}(\omega)$  and  $\hat{e}(\omega)$  are the transmission Fresnel factor and the polarization

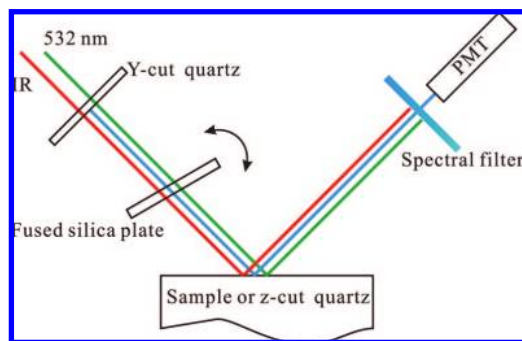


Figure 1. Schematic of the PS-SFVS setup.

unit vector of the beam at  $\omega$ , respectively. With  $\omega_{\text{IR}}$  near resonances, we can write

$$\vec{\chi}_S^{(2)} = \vec{\chi}_{\text{NR}}^{(2)} + \sum_q \frac{\vec{A}_q}{\omega_{\text{IR}} - \omega_q + i\Gamma_q} \quad (2)$$

if the resonances are discrete, and

$$\vec{\chi}_S^{(2)} = \vec{\chi}_{\text{NR}}^{(2)} + \int \frac{\vec{A}_q \rho(\omega_q)}{\omega_{\text{IR}} - \omega_q + i\Gamma_q} d\omega_q \quad (3)$$

if the resonances form a continuum. Here,  $\vec{\chi}_{\text{NR}}^{(2)}$  describes the nonresonant contribution.  $\vec{A}_q$ ,  $\omega_q$ , and  $\Gamma_q$  represent the amplitude, frequency, and damping constant of the  $q$ th vibrational resonance, respectively, and  $\rho(\omega_q)$  is the density of modes at  $\omega_q$ .

In general, it is difficult to properly deduce characteristics of the resonances from fitting a  $|\vec{\chi}_S^{(2)}|^2$  spectrum using eq 2 or 3 if the resonances strongly overlap or form a continuum. For characterization of the resonances, one would like to know  $\text{Im} \vec{\chi}_S^{(2)}$ , instead of  $|\vec{\chi}_S^{(2)}|^2$ . (Note that  $\vec{\chi}_{\text{NR}}^{(2)}$  is real and does not contribute to  $\text{Im} \vec{\chi}_S^{(2)}$ .) This requires knowledge of both the amplitude,  $|\vec{\chi}_S^{(2)}|$ , and the phase,  $\Phi_S$ , of  $\vec{\chi}_S^{(2)}$ , both of which should be obtained directly from measurement. It is clear that  $\Phi_S$  can be deduced from interference of the SF signal from the sample with that from a reference.

Depicted in Figure 1 is a possible scheme for the phase measurement of  $\vec{\chi}_S^{(2)}$ .<sup>21</sup> It involves insertion of a reference crystal and a phase plate in the incoming beam path of a SFVS setup using the collinear beam geometry. The SF output generated from both the reference and the sample is given by:<sup>21</sup>

$$S(\omega_{\text{IR}}) \propto |\chi_S^{(2)}(\omega_{\text{IR}}) + ae^{i\Phi} \chi_{\text{Ref}}^{(2)}(\omega_{\text{IR}})|^2 + b^2 |\chi_{\text{Ref}}^{(2)}(\omega_{\text{IR}})|^2 = |\chi_S^{(2)}(\omega_{\text{IR}})|^2 + (a^2 + b^2) |\chi_{\text{Ref}}^{(2)}(\omega_{\text{IR}})|^2 + 2a\chi_S^{(2)} \chi_{\text{Ref}}^{(2)} \cos[\Phi_S(\omega_{\text{IR}}) - \Phi_{\text{Ref}}(\omega_{\text{IR}}) - \Phi(\omega_{\text{IR}})] \quad (4)$$

where  $\chi_S^{(2)} = |\chi_S^{(2)}| e^{i\Phi_S}$ ,  $\chi_{\text{Ref}}^{(2)} = |\chi_{\text{Ref}}^{(2)}| e^{i\Phi_{\text{Ref}}}$ ,  $a\chi_{\text{Ref}}^{(2)}$  (with respect to  $\chi_S^{(2)}$ ) is the part of the reference SF field that overlaps and interferes with the sample SF field,  $(a^2 + b^2) |\chi_{\text{Ref}}^{(2)}|^2$  is the total reference SF signal, and  $\Phi$  is a relative phase that can be adjusted by the fused silica phase plate. Because  $|\chi_S^{(2)}(\omega_{\text{IR}}) + ae^{i\Phi} \chi_{\text{Ref}}^{(2)}(\omega_{\text{IR}})|^2 + b^2 |\chi_{\text{Ref}}^{(2)}(\omega_{\text{IR}})|^2$ ,  $|\chi_S^{(2)}(\omega_{\text{IR}})|^2$ , and  $(a^2 + b^2) |\chi_{\text{Ref}}^{(2)}|^2$  can be measured separately, and  $\Phi_{\text{Ref}}(\omega_{\text{IR}})$  is known, by measuring two sets of  $S(\omega_{\text{IR}})$  with different relative phases  $\Phi(\omega_{\text{IR}})$ ,  $\Phi_S(\omega_{\text{IR}})$  can be readily deduced. The spectra of  $\text{Re} \vec{\chi}_S^{(2)}(\omega_{\text{IR}})$  and  $\text{Im} \vec{\chi}_S^{(2)}(\omega_{\text{IR}})$  can then be obtained.

(19) Wei, X.; Miranda, P. B.; Shen, Y. R. *Phys. Rev. Lett.* **2001**, *86*, 1554–1557.

(20) Ostroverkhov, V.; Waychunas, G. A.; Shen, Y. R. *Phys. Rev. Lett.* **2005**, *94*, 046102/1–046102/4.

(21) Ji, N.; Ostroverkhov, V.; Chen, C. Y.; Shen, Y. R. *J. Am. Chem. Soc.* **2007**, *129*, 10056–10057.

(22) Ji, N.; Ostroverkhov, V.; Tian, C. S.; Shen, Y. R. *Phys. Rev. Lett.* **2008**, *100*, 096102/1–096102/4.

(23) Shen, Y. R. In *Frontier in Laser Spectroscopy*; Inguscio, T. W. H. A. M., Ed.; North Holland: Amsterdam, 1994; pp 139–165.

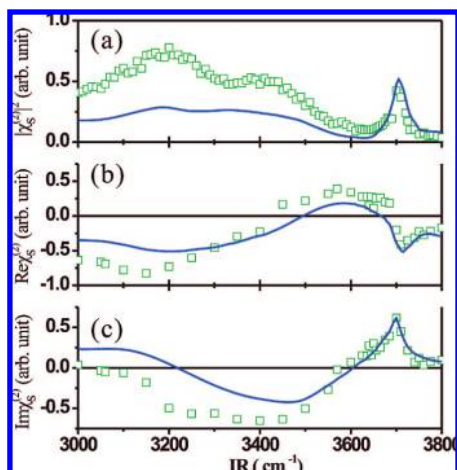


**Figure 2.** Spectra of (a)  $|\chi_S^{(2)}|^2$ , (b)  $\text{Re } \chi_S^{(2)}$ , and (c)  $\text{Im } \chi_S^{(2)}$  for the water/vapor interfaces of 1.2 M HCl solution (symbols) and neat water (lines).

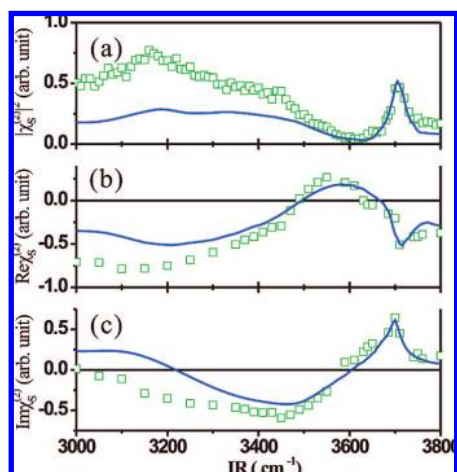


**Figure 3.** Spectra of (a)  $|\chi_S^{(2)}|^2$ , (b)  $\text{Re } \chi_S^{(2)}$ , and (c)  $\text{Im } \chi_S^{(2)}$  for the water/vapor interfaces of 1.2 M HI solution (symbols) and neat water (lines).

The details of our PS-SFVS setup are described in ref 21. As seen in Figure 1, a green beam (532 nm) and a tunable IR beam (2.5–3.6  $\mu\text{m}$ ) derived from a picosecond Nd:YAG laser/optical parametric amplifier system propagated collinearly through a  $y$ -cut quartz plate and then onto the sample at an incident angle of  $45^\circ$ . The beam diameter and energy at the sample were 0.2 mm and  $\sim 300 \mu\text{J/pulse}$  for the green input, and 0.1 mm and  $\sim 120 \mu\text{J/pulse}$  for the IR input. The SF signal generated from the  $y$ -cut quartz, serving as a reference, interfered with that from the sample in the reflected direction. The interference signal was detected by a photomultiplier/gated integrator system after spectral filtering. A fused silica phase plate inserted between the sample and the  $y$ -cut quartz was used to vary  $\Phi$ . The SF output was normalized against that from a  $z$ -cut quartz plate. The accuracy of our phase measurement was  $\sim 10^\circ$  at relatively low SF signal, but better at higher signal level.

The nonvanishing elements of  $\overline{\chi}_S^{(2)}$  for water/vapor interfaces are

$$\chi_{S,YYZ}^{(2)} = \chi_{S,XXZ}^{(2)}, \chi_{S,YZY}^{(2)} = \chi_{S,XZX}^{(2)}, \chi_{S,ZYY}^{(2)} = \chi_{S,ZXX}^{(2)} \text{ and } \chi_{S,ZZZ}^{(2)} \quad (5)$$

where  $Z$  is along the surface normal. We shall focus on  $\chi_{S,YYZ}^{(2)}$ , which can be measured by the SSP polarization combination

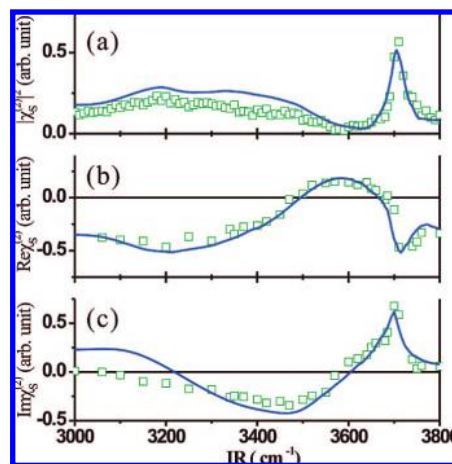


**Figure 4.** Spectra of (a)  $|\chi_S^{(2)}|^2$ , (b)  $\text{Re } \chi_S^{(2)}$ , and (c)  $\text{Im } \chi_S^{(2)}$  for the water/vapor interfaces of 1.2 M NaOH solution (symbols) and neat water (lines).

(denoting S-, S-, and P-polarized SF output, visible input, and IR input, respectively). We note that the SF signal is proportional to  $|\chi_{\text{eff}}^{(2)}|^2$ , and  $\chi_{\text{eff}}^{(2)}$  in eq 1 is related to  $\chi_S^{(2)}$  through the Fresnel factors that depend on the beam geometry. To avoid confusion and be able to compare our spectra with those reported in the literature, we shall present our spectra with the Fresnel factors removed; that is, we shall focus our discussion on  $\chi_S^{(2)}$  instead of  $\chi_{\text{eff}}^{(2)}$ .

Aqueous solutions were held in a glass cell. Beams interrogating the water/vapor interface went through holes in the top cover of the cell. In preparing the samples, the cell was soaked in strong acid (98%  $\text{H}_2\text{SO}_4$  + NoChromix) for more than 2 days, then rinsed thoroughly with distilled water (18.3 M $\Omega$  cm), and finally blow-dried with nitrogen gas. With such treatment, the sample surfaces were found free of detectable contaminants. Because HI in water is sensitive to room light, we prepared and kept the HI solution always in the dark.

## Results

We present in Figures 2–4 the measured spectra of  $|\chi_S^{(2)}|^2$ ,  $\text{Re } \chi_S^{(2)}$ , and  $\text{Im } \chi_S^{(2)}$ , for water/vapor interfaces of aqueous solutions of 1.2 M HCl, HI, and NaOH, respectively. For comparison, we also plotted in each figure the spectra for the neat water/vapor interface. (The sign of  $\text{Im } \chi_S^{(2)}$  describes the average polar orientation of the corresponding OH stretches with reference to  $\text{Im } \chi_S^{(2)}$  taken positive for the dangling OH bond at  $3700 \text{ cm}^{-1}$ .) In all cases, our  $|\chi_S^{(2)}|^2$  spectra, which have the Fresnel coefficients removed, agree well with those obtained by others.<sup>7,8,11</sup> The spectra of all cases appear qualitatively similar, all having an ice-like and a liquid-like feature peaked at  $\sim 3200$  and  $\sim 3400 \text{ cm}^{-1}$ . Comparison with the neat water case shows that both features are significantly enhanced for HCl and HI solutions and only weakly altered for NaOH solution. In contrast, the corresponding  $\text{Im } \chi_S^{(2)}$  spectra exhibit little changes above  $3500 \text{ cm}^{-1}$  in all cases, but significant changes below  $3450 \text{ cm}^{-1}$  for HCl and HI solutions, including a stronger negative liquid-like band for HCl and HI solutions, and a flip of sign in the ice-like region. Comparison of the  $\text{Im } \chi_S^{(2)}$  spectra for HCl and HI solutions shows a stronger negative strength for HCl in the  $\sim 3180$ – $3500 \text{ cm}^{-1}$  region and a stronger negative strength for HI in the  $\sim 3100$ – $3180 \text{ cm}^{-1}$  region. For the NaOH solution, the  $\text{Im } \chi_S^{(2)}$  spectrum is somewhat less negative between  $3200$  and  $3500 \text{ cm}^{-1}$  as compared to the neat

water case and shows a negative, but nearly vanishing, ice-like band below  $3200\text{ cm}^{-1}$ .

## Discussion

For water/vapor interfaces of HCl, HI, and NaOH solutions, the spectral changes observed in Figures 2–4 with respect to the neat water case must come from ions appearing at the interfaces. It is believed that  $\text{H}^+$ ,  $\text{I}^-$ , and perhaps also  $\text{OH}^-$  can preferentially reside at a water/vapor interface. They could disturb the interfacial hydrogen(H)-bonding structure of water either by their physical presence or by the surface field they create.<sup>7,8,12,18,24</sup>

In the following discussion, we shall use the neat water/vapor interface always as a reference. To facilitate the discussion, therefore, we need to briefly review the spectra and structure of the neat water/vapor interface deduced from our earlier PS-SFVS measurement.<sup>22</sup> We have found that while the  $|\chi_S^{(2)}|^2$  spectrum for neat water/vapor interface (displayed in Figures 2a, 3a, and 4a as reference) is the same as those reported by others, the  $\text{Im } \chi_S^{(2)}$  spectrum (in Figures 2c, 3c, and 4c) is very different from those of others obtained from fitting of the  $|\chi_S^{(2)}|^2$  spectrum.<sup>7,8</sup> The  $\text{Im } \chi_S^{(2)}$  spectrum allows us to construct a qualitative picture of the interfacial structure: The water surface appears as a highly distorted ice surface. The topmost layer is covered with DAA and DDA molecules. (Here, D and A denote donor and acceptor H-bonds, respectively, with which water molecules connect to the neighbors.)<sup>25</sup> The subsequent layer has DDAA molecules symmetrically or asymmetrically donor-bonded or singly donor-bonded to molecules in the topmost layer. The molecules in these two layers are largely responsible for the observed SF spectra because further down into the liquid, molecular ordering at the surface rapidly decays away and approaches that of the isotropic bulk. In the  $\text{Im } \chi_S^{(2)}$  spectrum, the sharp peak at  $3700\text{ cm}^{-1}$  can be identified as the OH stretch of the dangling OH at the surface, the  $3450\text{--}3700\text{ cm}^{-1}$  region mainly as donor-bonded OH stretches of DDA and DAA molecules, the  $3200\text{--}3450\text{ cm}^{-1}$  region mainly as asymmetrically donor-bonded DDAA molecules, and  $3000\text{--}3200\text{ cm}^{-1}$  regions mainly as symmetrically donor-bonded DDAA molecules. We emphasize here that the overall spectrum results from a continuous band of OH stretch resonances of interfacial water molecules that are H-bonded to neighbors with a wide variety of different geometries and strengths. Therefore, the above description is only a crude approximation. Molecules ascribed here to the specific spectral regions also contribute to some extent to the neighboring spectral regions. For example, both symmetrically and asymmetrically bonded DDAA molecules should contribute to the  $\text{Im } \chi_S^{(2)}$  spectrum around  $3200\text{ cm}^{-1}$ , one positively and the other negatively so that the combined  $\text{Im } \chi_S^{(2)}$  is nearly zero.

We now compare the spectra of water/vapor interfaces of aqueous solutions with those of neat water. The spectral change then allows us to learn how ions emerging at the interfaces perturb the interfacial structure. We consider first the HCl acid solution. It was found earlier that there was no detectable structural change of the water/vapor interface with addition of up to 1.7 M NaCl in water.<sup>26</sup> This indicates that both  $\text{Na}^+$  and

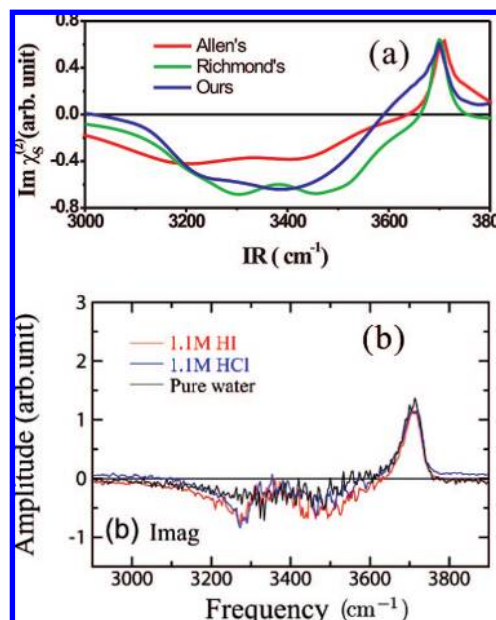


**Figure 5.** (a) Comparison of  $\text{Im } \chi_S^{(2)}$  spectra of the water/vapor interface of 1.2 M HCl solution obtained (or deduced from spectral information given) by different groups. (b)  $\text{Im } \chi_S^{(2)}$  spectra obtained by MD simulation of Ishiyama and Morita presented in ref 12.

$\text{Cl}^-$  are largely repelled from the interface. In HCl solution, however, protons are likely to be concentrated at the interface as suggested by molecular dynamics simulations.<sup>9–11</sup> They can be readily incorporated into the interfacial H-bonding network as hydrated ions in the form of  $\text{H}_3\text{O}^+$  (Eigen form, hydronium) and/or  $\text{H}_5\text{O}_2^+$  (Zundel form,  $\text{H}_2\text{O}\text{--}\text{H}\text{--}\text{OH}_2^+$ ).<sup>7,8,11,18</sup> These hydrated ions can influence the interfacial spectra directly through their own OH stretches and less directly through reorientation of interfacial water molecules by the surface field they create. Recent SFVS studies<sup>7</sup> showed enhancement of both ice-like and liquid-like bands in the  $|\chi_S^{(2)}|^2$  spectrum due to solvation of HCl in water, which was an indication that  $\text{H}^+$  ions had emerged at the interface to modify the water interfacial structure. Shultz and co-workers understood the enhancement as due to reorientation of interfacial water molecules by the  $\text{H}^+\text{--}\text{Cl}^-$  created surface field.<sup>18</sup> Richmond and co-workers decomposed the  $|\chi_S^{(2)}|^2$  spectrum into discrete resonances and attributed the enhancement of the  $3200$  and  $3330\text{ cm}^{-1}$  modes to effects of the strong surface field and strong electrostatic interactions between hydrated protons ( $\text{H}_3\text{O}^+$  and  $\text{H}_5\text{O}_2^+$ ) and water molecules at the interface.<sup>7</sup> Allen and co-workers fitted the spectrum with a different set of discrete resonances and suggested that the enhancement at  $3200\text{ cm}^{-1}$  came from the surface field effect as well as contributions from OH stretch vibrations of  $\text{H}_3\text{O}^+$  and  $\text{H}_5\text{O}_2^+$  at the interface.<sup>8,11</sup> Ishiyama and Morita recently reported their MD simulations on the water/vapor interface of HCl solution.<sup>12</sup> Their calculated  $|\chi_S^{(2)}|^2$  spectrum agrees qualitatively with the experimental one, and the calculated  $\text{Im } \chi_S^{(2)}$  spectrum also resembles that deduced from decomposition of the  $|\chi_S^{(2)}|^2$  spectrum by Richmond's group.<sup>7</sup> (See Figure 5, where we compare the  $\text{Im } \chi_S^{(2)}$  spectra obtained by different groups. The signs of the resonant amplitudes were not specified in ref 7. In composing the  $\text{Im } \chi_S^{(2)}$  spectrum from the information given in ref 7, we assume that all of the bonded OH modes have negative amplitude as we have measured.)

Our  $|\chi_S^{(2)}|^2$  spectrum in Figure 2a for the water/vapor interface of a 1.2 M HCl solution is essentially the same as that obtained

(24) Liu, D. F.; Ma, G.; Levering, L. M.; Allen, H. C. *J. Phys. Chem. B* **2004**, *108*, 2252–2260.

(25) Buck, U.; Ettischer, I.; Melzer, M.; Buch, V.; Sadlej, J. *Phys. Rev. Lett.* **1998**, *80*, 2578–2581.

(26) Raymond, E. A.; Richmond, G. L. *J. Phys. Chem. B* **2004**, *108*, 5051–5059.

by other groups, but the measured  $\text{Im } \chi_S^{(2)}$  spectrum is different from those of others deduced from the  $|\chi_S^{(2)}|^2$  spectrum assuming discrete resonances,<sup>7,8</sup> and also from that of MD simulation,<sup>12</sup> as shown in Figure 5. (We note that significant differences in amplitude and sign also exist between our directly measured  $\text{Im } \chi_S^{(2)}$  spectrum and those of others for the neat water/vapor interface.) In comparison with the spectrum of the neat water/vapor interface also displayed in Figure 2c, the dangling OH peak at  $\sim 3700 \text{ cm}^{-1}$  hardly changes, but the broadband due to bonded OH stretches in the  $|\chi_S^{(2)}|^2$  spectrum is significantly enhanced. From the spectra of  $\text{Re } \chi_S^{(2)}$  and  $\text{Im } \chi_S^{(2)}$ , it is obvious that the enhancement in the higher frequency region ( $\geq 3200 \text{ cm}^{-1}$ ) comes from enhancement of  $\text{Im } \chi_S^{(2)}$  and enhancement in the lower frequency region ( $\leq 3250 \text{ cm}^{-1}$ ) comes from  $\text{Re } \chi_S^{(2)}$ .

The  $\text{Im } \chi_S^{(2)}$  spectra are more informative because they directly reflect the resonance profiles as described in eq 3. Comparing the  $\text{Im } \chi_S^{(2)}$  spectra of HCl solution and neat water, we find (1) there is hardly any change above  $3500 \text{ cm}^{-1}$ , (2) the negative liquid-like band between  $3200$  and  $\sim 3450 \text{ cm}^{-1}$  becomes significantly stronger for the HCl solution, and (3) the ice-like band below  $3200 \text{ cm}^{-1}$  flips from positive to negative with HCl in water and terminates at  $\sim 3100 \text{ cm}^{-1}$ .

Using the  $\text{Im } \chi_S^{(2)}$  spectrum in relation to the structure of neat water/vapor interface as references, we can deduce information from the spectral changes on how the interfacial structure of the HCl solution differs from that of neat water. As mentioned earlier,  $\text{H}^+$  likes to emerge at the interface. Knowing that the spectrum above  $3500 \text{ cm}^{-1}$  comes mainly from DAA and DDA water molecules in the topmost layer at the surface, its insignificant change indicates that the surface concentration of  $\text{H}^+$  or hydrated  $\text{H}^+$  is not high enough to physically perturb the structure of the topmost layer. This is supported by the result of MD simulation that the excess proton concentration at the surface should be less than 4% of a monolayer.<sup>12</sup> The surface field created by interfacial  $\text{H}^+$  ions cannot affect DAA and DDA molecules in the topmost layer, but can reorient the more loosely H-bonded DDAA molecules in the adjacent layer with  $\text{O} \rightarrow \text{H}$  toward the bulk liquid, thus enhancing the negative liquid-like band between  $3200$  and  $3500 \text{ cm}^{-1}$ . It is less likely to be able to reorient DDAA molecules contributing to the ice-like band because of their stronger H-bonding to neighbors.<sup>27</sup> The observed flip of the ice-like band below  $3200 \text{ cm}^{-1}$  from positive to negative could be due to contribution of OH stretches of hydronium ( $\text{H}_3\text{O}^+$ ) ions appearing at the interface. They have preferred orientation with  $\text{O} \rightarrow \text{H}$  pointing into the liquid and therefore contribute negatively to the respective spectral region. In recent years, there has been a great deal of discussion on the existence of hydronium ions and their OH stretch frequencies. Infrared spectroscopic studies on clusters ( $n = 5$ )<sup>28</sup> and bulk HCl solutions<sup>29</sup> suggest the presence of hydronium ions with a stretch frequency around  $\sim 2900 \text{ cm}^{-1}$ . Raman studies found a very broad band (called proton continuum) below  $\sim 3200 \text{ cm}^{-1}$ ,

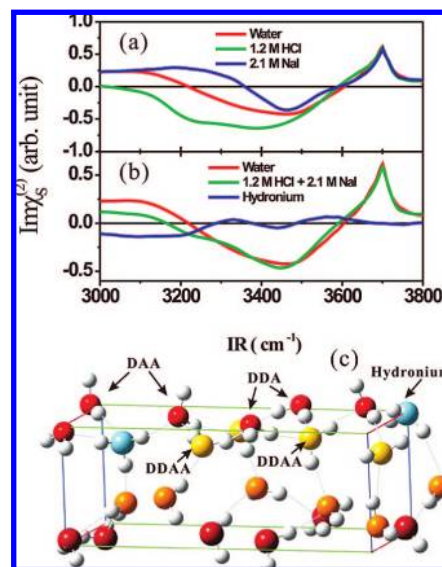


**Figure 6.** (a)  $\text{Im } \chi_S^{(2)}$  spectra of water/vapor interfaces of neat water (red line), 1.2 M HCl solution (green line), and 2.1 M NaI solution (blue line). (b)  $\text{Im } \chi_S^{(2)}$  spectrum of water/vapor interfaces of neat water (red line), average of  $\text{Im } \chi_S^{(2)}$  spectra for 1.2 M HCl and 2.1 M NaI solutions (green line), and the difference spectrum deduced from the above two (blue line). (c) Cartoon depicting the water/vapor interfacial structure of the HCl solution with hydronium ions (oxygen painted blue) close to the surface. Water molecules in different interfacial layers have their oxygen coded with different colors: DAA and DDA molecules in the topmost layer colored with red, DDAA molecules in the second layer colored with gold, and DDAA molecules in the third and fourth layers colored with orange and red, respectively.

which was attributed to  $\text{H}_3\text{O}^+$  and  $\text{H}_5\text{O}_2^+$ .<sup>8,30</sup> The spectral change we observe in the ice-like band region suggests that the surface hydronium ions do exist and should have their OH stretch frequencies in the range of  $3000$ – $3250 \text{ cm}^{-1}$ . It is possible that hydronium ions at the interface with no acceptor bond and weaker donor bonds to neighbors would have higher OH stretch frequencies than in the bulk.

To check the validity of the above assignment, we tried to single out contribution from hydronium to the spectrum by removing the contribution from the surface field effect, assuming the two contributions to the spectral change in  $\text{Im } \chi_S^{(2)}$  appeared in linear superposition. This can be done by comparing the spectrum of neat water with a linear combination of spectra for HCl and NaI solutions. From previous SFVS studies of NaI solution,<sup>22</sup> it is known that  $\text{I}^-$  ions prefer to come to the surface and create a negative surface field. The spectral change in  $\text{Im } \chi_S^{(2)}$  with respect to the neat water interface mainly comes from the surface field reorienting the interfacial DDAA water molecules.<sup>22</sup> On the other hand, in HCl solution, the surface field created by excess  $\text{H}^+$  is positive and induces a spectral change opposite to that in NaI solution. Thus, if we choose a proper linear combination of the two spectra for HCl and NaI solutions, we can expect cancellation of the surface field effect in the combined spectrum. Then, in comparing the combined spectrum with that of neat water, the observed difference would have to come from OH stretches of the hydronium ions. In Figure 6a, we show separately the  $\text{Im } \chi_S^{(2)}$  spectra for 1.2 M HCl and 2.1 M NaI solutions. The two are obviously different in the  $3000$ – $3500 \text{ cm}^{-1}$  region. We then present in Figure 6b the combined  $\text{Im } \chi_S^{(2)}$  spectrum composed of a 1:1 linear

(27) In a previous study on a 2.1 M NaI solution [ref 22], it was found that the surface field created by  $\text{I}^-$  ions emerging at the surface was not strong enough to alter the spectrum below  $3200 \text{ cm}^{-1}$  significantly. The surface field created by protons at the surface in a 1.2 M HCl solution is not expected to be stronger.

(28) Headrick, J. M.; Diken, E. G.; Walters, R. S.; Hammer, N. I.; Christie, R. A.; Cui, J.; Myshakin, E. M.; Duncan, M. A.; Johnson, M. A.; Jordan, K. D. *Science* **2005**, *308*, 1765–1769.

(29) Kim, J.; Schmitt, U. W.; Gruetzmacher, J. A.; Voth, G. A.; Scherer, N. E. *J. Chem. Phys.* **2002**, *116*, 737–746.

(30) Kanno, H. *J. Raman Spectrosc.* **1993**, *24*, 689–693.

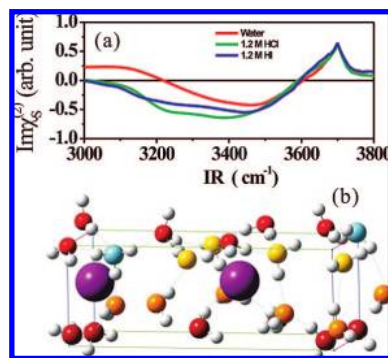


**Figure 7.** (a) Comparison of  $\text{Im } \chi_S^{(2)}$  spectra of water/vapor interfaces of neat water (red line), 1.2 M HCl (green line), and HI (blue line) solutions. (b) Cartoon depicting the water/vapor interfacial structure of the HI solution. The color codes for interfacial water molecules in different layers are the same as those given in Figure 6. Oxygens of hydronium ions close to the surface are painted blue, and iodine ions are painted purple.

combination of the two spectra displayed in Figure 6a for the 1.2 M HCl and 2.1 M NaI solutions and compare it with that of neat water. The two spectra in Figure 6b appear to differ appreciably only below  $3250 \text{ cm}^{-1}$ ; indeed, the surface field effect that affects mainly the spectral region  $3200\text{--}3500 \text{ cm}^{-1}$  has been nearly suppressed. The difference spectrum of the two, also shown in Figure 6b, displays a negative band below  $3250 \text{ cm}^{-1}$  that can be attributed to OH stretches of interfacial hydronium ions. Figure 6c shows a cartoon describing the water/vapor interfacial structure of HCl solution.

We next consider the water/vapor interface of the HI acid solution. Both  $\text{H}^+$  and  $\text{I}^-$  would have excess at the surface. However,  $\text{H}^+$  must have more surface excess because, as we described earlier, it takes 2.1 M NaI in water to produce enough surface excess  $\text{I}^-$  ions to create the same field strength as that of surface excess  $\text{H}^+$  ions produced by 1.2 M HCl. For an HI solution with equal bulk concentrations of  $\text{H}^+$  and  $\text{I}^-$ , more  $\text{H}^+$  than  $\text{I}^-$  must appear at the water/vapor interface. This is supported by MD simulation.<sup>12</sup> The surface ions form a double-charge layer with a positive surface field that could reorient DDAA molecules with  $\text{O}\rightarrow\text{H}$  pointing toward the liquid bulk and enhance the negative liquid-like band in the  $\text{Im } \chi_S^{(2)}$  spectrum.

Our  $|\chi_S^{(2)}|^2$  spectrum for the 1.2 M HI solution in Figure 3a is the same as those obtained by others, but our  $\text{Im } \chi_S^{(2)}$  spectrum is again different from those of others deduced from fitting of the  $|\chi_S^{(2)}|^2$  spectrum.<sup>8</sup> As compared to that of neat water, the  $\text{Im } \chi_S^{(2)}$  spectrum of the HI solution shows little change above  $3500 \text{ cm}^{-1}$ , but displays an enhanced negative strength in the  $3200\text{--}3500 \text{ cm}^{-1}$  liquid-like region and a negative ice-like band below  $3200 \text{ cm}^{-1}$ . This result supports the picture that more  $\text{H}^+$  than  $\text{I}^-$  appear at the surface, producing a positive surface field that changes the liquid-like spectral feature through reorientation of the asymmetrically bonded DDAA water molecules. This picture differs from the one predicted by MD simulation of Dang et al.<sup>4</sup> that shows a negative surface field formed by  $\text{H}^+$  and  $\text{I}^-$ , but agrees with the MD simulations of Morita et al.<sup>12</sup> In addition to the surface field effect, the hydronium ions formed by  $\text{H}^+$  at the interface again contribute directly to the spectrum below  $3200 \text{ cm}^{-1}$ , making the ice-like band appear negative.

As compared to the  $\text{Im } \chi_S^{(2)}$  spectrum of the 1.2 M HCl solution (see Figure 7a), the enhancement in the liquid-like region of the HI case is somewhat less, but the negative ice-

like band is stronger. This is an indication that there are more hydronium ions at the interface of the HI solution than of the HCl solution, but the surface field effect is weaker. We can understand the observation as follows. Because of Coulomb interaction, the presence of  $\text{H}^+$  (or hydronium ions) at the interface helps attract  $\text{I}^-$  ions to the interface and vice versa.<sup>31</sup> Therefore, for the same molar concentration of HI, HCl, and NaI in solutions, more  $\text{H}^+$  and  $\text{I}^-$  ions are expected at the interface of the HI solution than  $\text{H}^+$  and  $\text{I}^-$  ions at the interfaces of the HCl and NaI solutions, respectively. Saykally and co-workers used second harmonic generation to monitor the amount of  $\text{I}^-$  ions at the vapor/water interfaces of NaI and HI solutions, and indeed found more  $\text{I}^-$  ions in the HI case.<sup>31</sup> However, because both  $\text{H}^+$  and  $\text{I}^-$  preferentially appear at the surface, they are likely to be close to each other, forming a relatively thin double-charge layer. As compared to the HCl case, even though the surface concentration of  $\text{H}^+$  is higher, the overall surface field effect could still be weaker because of the thinner double-charge layer, as actually seen from the weaker liquid-like band in the  $\text{Im } \chi_S^{(2)}$  spectra. MD simulations support the above description.<sup>11,12</sup> Morita et al. show that the HI solution has a larger surface excess density of  $\text{H}^+$  ( $\rho/\rho_{\text{bulk}} = 2.3$ ) than the HCl solution ( $\rho/\rho_{\text{bulk}} = 1.55$ ), but the average gap between  $\text{H}^+$  and  $\text{I}^-$  is only  $1.5 \text{ \AA}$ , much smaller than that between  $\text{H}^+$  and  $\text{Cl}^-$  ( $4.5 \text{ \AA}$ ). Thus, the surface potential is lower at the interface of the HI solution. We present in Figure 7b a cartoon describing the interfacial water structure of the HI solution.

Finally, we consider the water/vapor interface of 1.2 M NaOH solution. This is a case more difficult to understand. Even in the bulk, how  $\text{OH}^-$  is incorporated in an hydrogen-bonding structure of water is not very clear.<sup>32</sup> Traditionally,  $\text{OH}^-$  is thought of being a “mirror image” of  $\text{H}^+$  in water, capable of hydrogen-bonding to four neighboring water molecules by three acceptor bonds and one donor bond. However, this picture has been challenged by recent theoretical and experimental works, which proposed that  $\text{OH}^-$  could have one donor and four acceptor bonds.<sup>32,33</sup> The bonding structure of  $\text{OH}^-$  at the water/vapor interface is even less clear. MD simulation predicts that  $\text{OH}^-$  should be repelled from the interface.<sup>11</sup> SFVS studies on 1.3 M NaOH solution, on the other hand, found clear reduction of the liquid-like band in the  $|\chi_S^{(2)}|^2$  spectrum,<sup>7,11</sup> indicating that  $\text{OH}^-$  had emerged at the interface. The reduction was attributed to  $\text{OH}^-$  inducing random orientation of water molecules at the interface.<sup>7</sup>

Our  $|\chi_S^{(2)}|^2$  spectrum of 1.2 M NaOH in Figure 4 is the same as those of others seeing a reduction of the liquid-like band, but the  $\text{Im } \chi_S^{(2)}$  spectrum in comparison with the neat water case shows more clearly a change in the disappearance of the ice-like band below  $3200 \text{ cm}^{-1}$ , in addition to the weak reduction of the negative liquid-like band. The latter can be understood to be due to the surface field effect created by excess  $\text{OH}^-$  at the interface that tends to reorient interfacial water molecules with  $\text{O}\rightarrow\text{H}$  toward the interface. This rather small change, in comparison with those observed in NaI, HCl, and HI solutions, indicates that the field resulting from surface excess of  $\text{OH}^-$  is much less than in the other cases, but it is still opposite to the prediction of MD simulation that there should be a surface

(31) Petersen, P. B.; Saykally, R. J. *J. Phys. Chem. B* **2005**, *109*, 7976–7980.

(32) Tuckerman, M. E.; Chandra, A.; Marx, D. *Acc. Chem. Res.* **2006**, *39*, 151–158.

(33) Botti, A.; Bruni, F.; Imberti, S.; Ricci, M. A.; Soper, A. K. *J. Mol. Liq.* **2005**, *117*, 81–84.

depletion of  $\text{OH}^-$ . The disappearance of the ice-like band must also be due to appearance of  $\text{OH}^-$  at the interface. It is not likely that the weak surface field can reorient the symmetrically bonded DDAA water molecules responsible for the ice-like band and is presumably the result of how  $\text{OH}^-$  is incorporated into the hydrogen-bonding structure of water at the interface. Randomization of interfacial structure by five-coordinated  $\text{OH}^-$  probably is not the reason because changes in other spectral regions are very weak. Because DDAA molecules symmetrically donor-bonded to the topmost DDA and DAA molecules mainly contribute to the ice-like band in the neat water case, we suspect that in NaOH solution,  $\text{OH}^-$  ions may have come to the interface to replace such DDAA molecules and thus reduce the ice-like band. It is also possible that incorporation of  $\text{OH}^-$  ions in the interfacial hydrogen-bonding structure may affect the OH stretches of water molecules bonded to them and contribute to the change of the ice-like band. However, these are pure conjectures. Theoretical help is clearly needed to understand the interfacial structure of NaOH solution.

### Conclusions

We used the PS-SFVS technique to study water/vapor interfaces of 1.2 M HCl, HI, and NaOH solutions, and obtained in the OH stretch region not only the  $|\chi_s^{(2)}|^2$  spectrum, but also the spectra of  $\text{Re } \chi_s^{(2)}$  and  $\text{Im } \chi_s^{(2)}$ . The  $\text{Im } \chi_s^{(2)}$  spectrum directly reveals the resonance characteristics and is therefore more informative. While our  $|\chi_s^{(2)}|^2$  spectra are essentially identical to those obtained by others, our  $\text{Im } \chi_s^{(2)}$  spectra are different from those deduced from fitting of the  $|\chi_s^{(2)}|^2$  spectra by others. Accordingly, our understanding of the water interfacial structures of these solutions is also different.

With the neat water/vapor interface taken as a reference, we found that protons in HCl solution like to appear in the form of hydronium ions at the interface and create a positive surface

field, which tends to reorient the interfacial water molecules and alters the liquid-like band of the spectrum. The hydronium ions themselves oriented with  $\text{O}\rightarrow\text{H}$  toward the liquid contribute to the negative ice-like band in the  $\text{Im } \chi_s^{(2)}$  spectrum. In the case of HI solution, both  $\text{H}^+$  and  $\text{I}^-$  prefer to appear at the interface. They form a double-charge layer, creating again a positive surface field that changes the liquid-like band in the spectrum. The hydronium ions at the interface also affect the spectrum the same way as in the HCl case. For the NaOH solution, the  $\text{Im } \chi_s^{(2)}$  spectrum indicates preferential appearance of  $\text{OH}^-$  at the interface, contrary to the prediction of MD simulation. How  $\text{OH}^-$  gets incorporated in the hydrogen-bonding structure of the water interface and alters the spectrum is, however, difficult to visualize.

This work demonstrates how PS-SFVS is needed to study water interfaces. The experimentally determined  $\text{Im } \chi_s^{(2)}$  spectrum properly describes the extremely broadband of OH stretch resonances originating from continuously varying bonding geometry and strength interfacial water molecules connect with neighbors. It presents more of a challenge to theoretical studies of water interfaces. Hopefully, theoretical reproduction of the spectrum could provide information on how different interfacial water species contribute to different spectral regions. Results from this work could also be used as the basis and references for future studies of other water interfaces including water/liquid and water/solid interfaces.

**Acknowledgment.** This work was supported by the NSF Science and Technology Center of Advanced Materials for Purification of Water with Systems (Water CAMPWS; CTS-0120978). N.J., G.A.W., and Y.R.S. also acknowledge support from the Department of Energy under Contract No. DE-AC03-76SF00098.

JA8021297